Rydberg Atoms and Optical Tweezers

Lecture Notes with Derivations

Contents

1 Why Neutral Atoms? 3

2 Rydberg Atoms: Basic Physics 3

2.1 Definition and Scaling 3

2.2 Why Strong Interactions Appear 4

3 Rydberg Blockade and Collective Excitation 5

3.1 Two-Atom Model 5

3.2 Blockade Condition 6

3.3 Derivation of the Blockade Radius 6

4 Cooling, Magneto-Optical Trapping, and Loading 7

4.1 Radiation Pressure and Scattering Force 7

4.2 Doppler Cooling Limit 8

4.3 Magneto-Optical Trap (MOT) 8

4.4 Why the MOT Must Be Followed by Tweezers 9

4.5 Loading from the MOT into Optical Tweezers 10

5 Optical Tweezers: Physical Basis 10

5.1 Dipole Interaction and AC Stark Shift 10

5.2 Rewriting the Potential in Terms of Intensity 10

5.3 Far-Detuned Two-Level Approximation 11

5.4 Derivation of the Useful Scaling 11

6 Gaussian Beam Model of a Tweezer 12

6.1 Intensity Distribution 12

6.2 Harmonic Approximation Near the Trap Minimum 12

6.3 Axial Trap Frequency 13

7 Quantum Motion in the Tweezer **14**

7.1 Lamb-Dicke Regime 14

8 Heating, Scattering, and Technical Noise **14**

9 Tweezer Arrays: From One Trap to Many **15**

9.1 Defect-Free Rearrangement 15

10 Single-Qubit and Rydberg-Coupled Dynamics **16**

10.1 Two-Level Driven Atom 16

10.2 Controlled Phase from Blockade 16

11 Quantum Computing with Rydberg Atoms **16**

11.1 Qubit Encoding 17

11.2 Why Rydberg Excitation Enables Two-Qubit Gates 17

11.3 Controlled-Phase Gate Idea 18

11.4 Minimal Physical Picture of a Blockade Gate 18

11.5 Why the Platform Scales Well 19

11.6 Analog and Digital Operation 19

11.7 Strengths and Challenges 19

11.8 Conceptual Summary 20

12 References **20**

1. Why Neutral Atoms?

Neutral-atom platforms combine long internal-state coherence, optical control, and the ability to scale to large arrays. The modern architecture is conceptually simple:

1. cool atoms in a magneto-optical trap,
2. load them into tightly focused optical tweezers,
3. rearrange atoms into defect-free arrays,
4. encode qubits in long-lived ground states,
5. switch on strong, controllable interactions through Rydberg excitation.

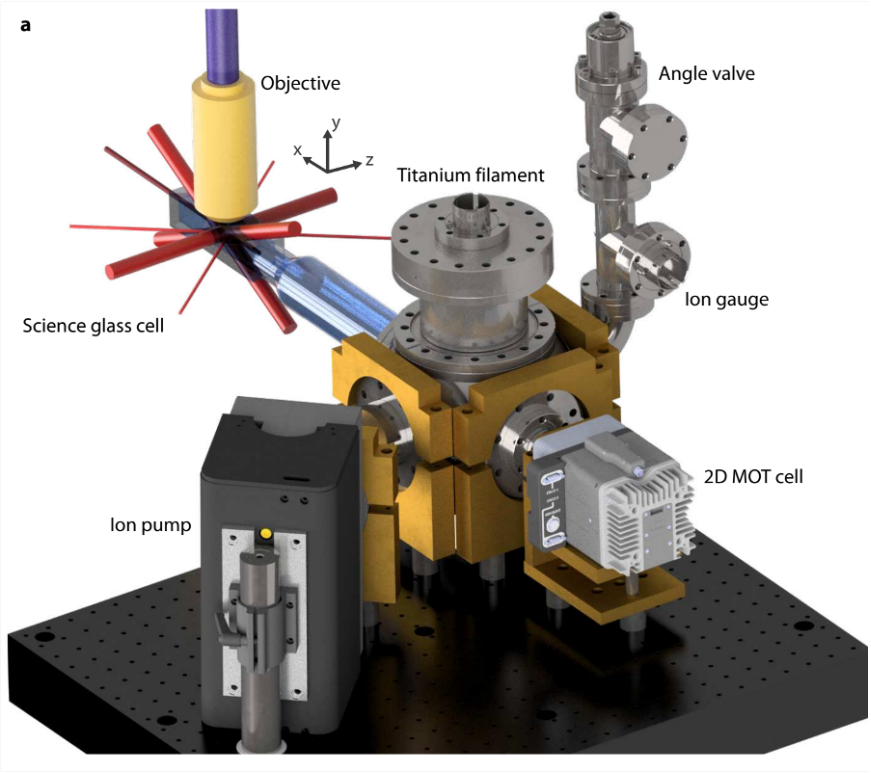

Remark

It is useful to ask three questions: (i) how do we hold one atom in space, (ii) how do we coherently drive it to a Rydberg state, and (iii) what changes when a second nearby atom is present?

2. Rydberg Atoms: Basic Physics

2.1 Definition and Scaling

A Rydberg atom is an atom with one valence electron excited to a very large principal quantum number $n \gg 1$. In a hydrogenic picture,

$$E_n = -\frac{Ry}{n^2}, \tag{1}$$

where Ry is the Rydberg energy. Several important quantities scale strongly with n:

$$\text{radius} \sim n^2 a_0, \tag{2}$$

$$\text{dipole matrix element} \sim n^2 e a_0, \tag{3}$$

$$\text{polarizability} \sim n^7, \tag{4}$$

$$\text{lifetime} \sim n^3, \tag{5}$$

$$\text{van der Waals coefficient } C_6 \sim n^{11}. \tag{6}$$

These extreme scalings are the reason Rydberg atoms are useful for quantum information: two atoms separated by a few micrometers can interact far more strongly in a Rydberg state than in their ground states.

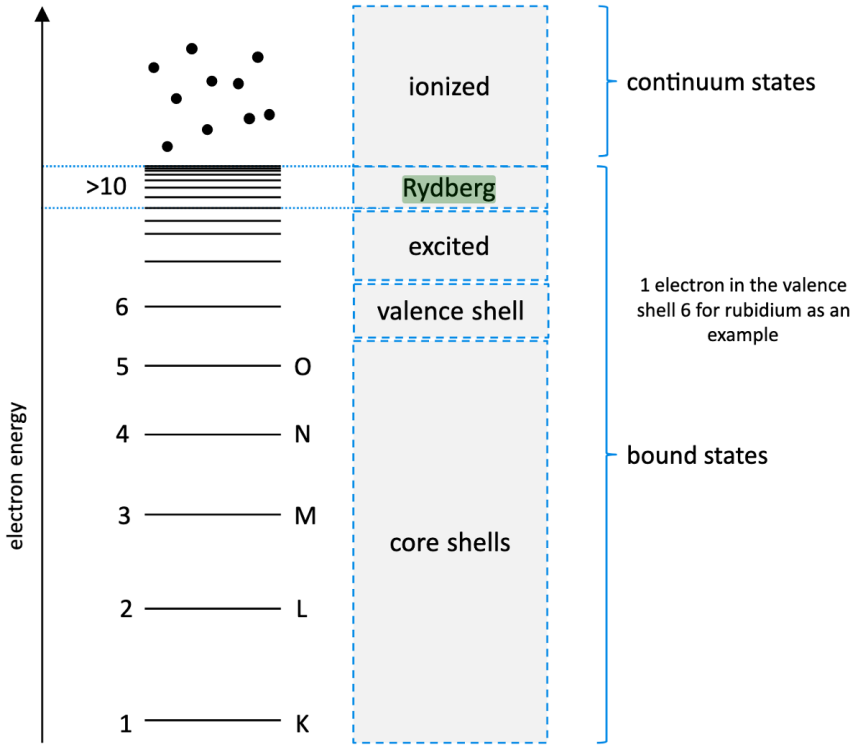

2.2 Why Strong Interactions Appear

Consider two atoms in Rydberg states. Their interaction can often be modeled as either resonant dipole-dipole or off-resonant van der Waals:

$$V_{dd}(R) = \frac{C_3}{R^3}, \tag{7}$$

$$V_{vdW}(R) = \frac{C_6}{R^6}. \tag{8}$$

Here R is the interatomic separation. The relevant form depends on whether nearby pair states are nearly degenerate. For many gate and blockade experiments, the effective interaction is van der Waals over the experimental distance scale.

Physical Insight

The crucial message is not only that the interaction is large, but that it is *switchable*. Atoms interact weakly in their ground states and strongly only when optically promoted to Rydberg states.

3. Rydberg Blockade and Collective Excitation

3.1 Two-Atom Model

Let $|g\rangle$ denote a ground state and $|r\rangle$ a Rydberg state. For two atoms, the basis is

$$\{|gg\rangle, |gr\rangle, |rg\rangle, |rr\rangle\}. \tag{9}$$

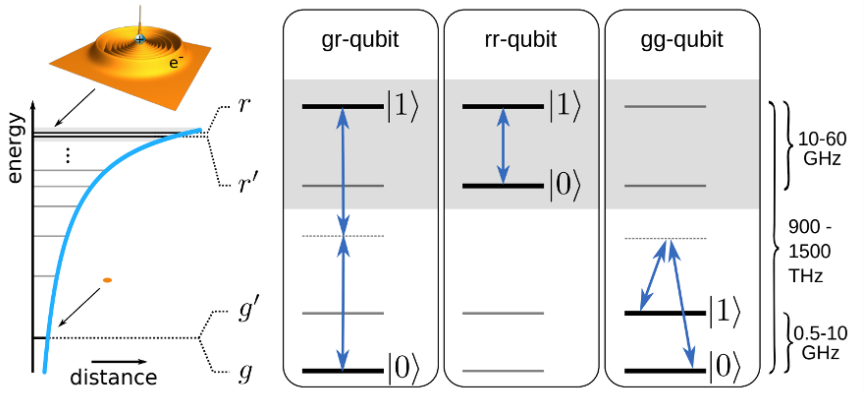

Suppose each atom is resonantly driven with Rabi frequency Ω. In the rotating-wave approximation, the two-atom Hamiltonian is

$$H = \frac{\hbar\Omega}{2}\Big(|gr\rangle\langle gg| + |rg\rangle\langle gg| + |rr\rangle\langle gr| + |rr\rangle\langle rg| + \text{h.c.}\Big) - \hbar\Delta\Big(|gr\rangle\langle gr| + |rg\rangle\langle rg| + 2|rr\rangle\langle rr|\Big) + V(R)\,|rr\rangle\langle rr|. \tag{10}$$

Here Δ is the detuning of the excitation laser from the atomic transition. It is useful to define the symmetric singly excited state

$$|W\rangle = \frac{1}{\sqrt{2}}\left(|gr\rangle + |rg\rangle\right). \tag{11}$$

Then the laser couples $|gg\rangle$ to $|W\rangle$ with enhanced Rabi frequency $\sqrt{2}\Omega$.

The orthogonal antisymmetric state

$$|D\rangle = \frac{1}{\sqrt{2}}(|gr\rangle - |rg\rangle) \tag{12}$$

is not coupled by the driving field and is therefore a dark state.

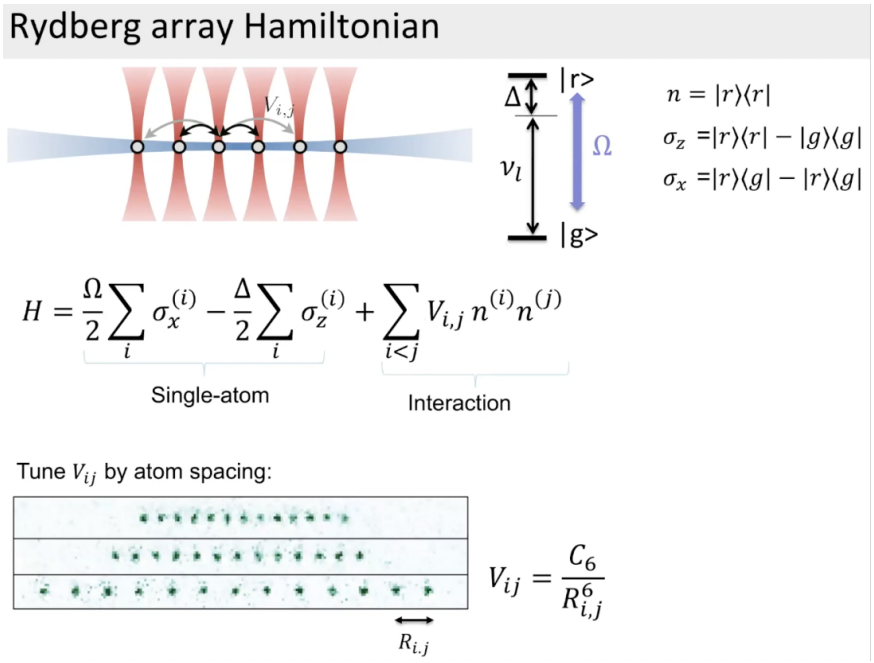

3.2 Blockade Condition

If the doubly excited state $|rr\rangle$ is shifted by interaction energy $V(R)$, then simultaneous excitation is suppressed whenever

$$V(R) \gg \hbar\Omega. \tag{13}$$

For a van der Waals interaction $V(R) = C_6/R^6$, the blockade radius is defined by

$$\frac{C_6}{R_b^6} = \hbar\Omega, \tag{14}$$

so that

$$R_b = \left(\frac{C_6}{\hbar\Omega}\right)^{1/6}. \tag{15}$$

3.3 Derivation of the Blockade Radius

The definition is simply the distance at which interaction energy becomes comparable to the resonant linewidth set by the Rabi drive. Starting from

$$V(R) = \frac{C_6}{R^6}, \tag{16}$$

set $V(R_b) = \hbar\Omega$:

$$\frac{C_6}{R_b^6} = \hbar\Omega. \tag{17}$$

Multiplying both sides by R_b^6 gives

$$C_6 = \hbar\Omega R_b^6, \tag{18}$$

and therefore

$$R_b^6 = \frac{C_6}{\hbar\Omega} \quad \Rightarrow \quad R_b = \left(\frac{C_6}{\hbar\Omega}\right)^{1/6}. \tag{19}$$

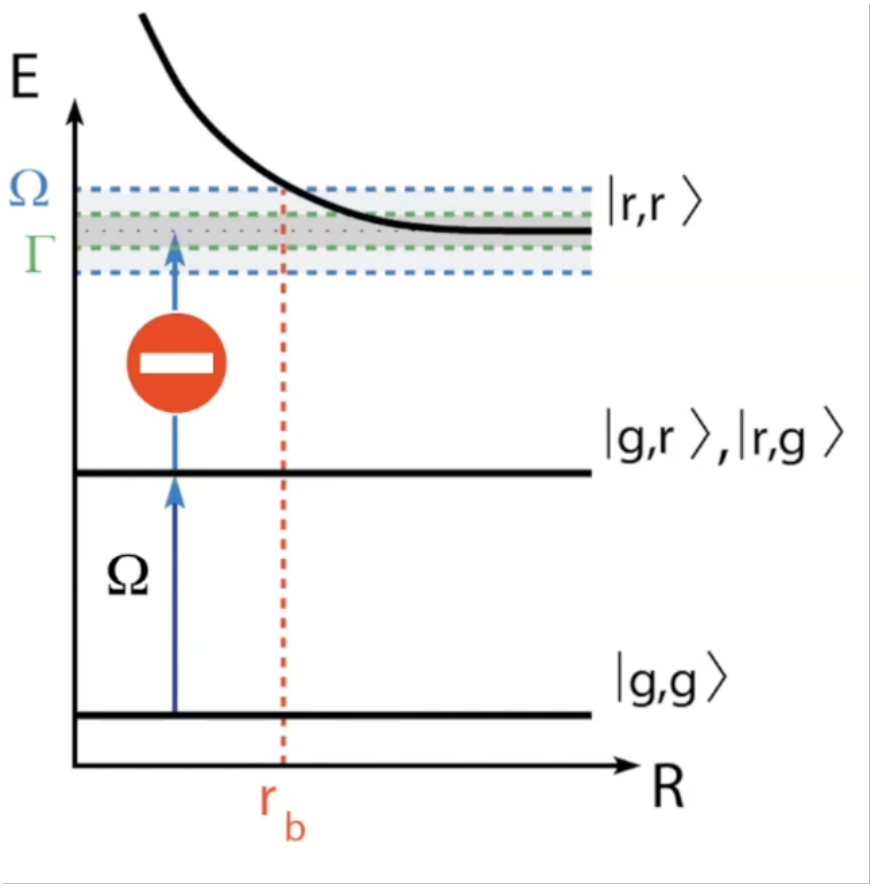

4. Cooling, Magneto-Optical Trapping, and Loading

Before atoms can be trapped in tightly focused optical tweezers and coherently excited to Rydberg states, they must first be cooled and spatially localized. In a typical neutral-atom experiment, the preparation sequence is:

1. produce a dilute atomic vapor or beam,
2. slow and cool the atoms with near-resonant laser light,
3. capture them in a magneto-optical trap (MOT),
4. optionally apply sub-Doppler cooling,
5. load atoms from the cold cloud into optical tweezers.

Remark

The MOT is not the final trapping stage used for quantum logic. Its role is to produce a cold and localized atomic reservoir from which individual tweezers can capture atoms.

4.1 Radiation Pressure and Scattering Force

Consider a two-level atom illuminated by near-resonant light of angular frequency ω, detuned from the atomic transition frequency ω_0 by

$$\Delta = \omega - \omega_0. \tag{20}$$

The saturation parameter is

$$s_0 = \frac{I}{I_{\text{sat}}}, \tag{21}$$

where I_{sat} is the saturation intensity. The photon scattering rate is

$$R_{\text{sc}} = \frac{\Gamma}{2} \frac{s_0}{1 + s_0 + (2\Delta/\Gamma)^2}, \tag{22}$$

with Γ the natural linewidth.

Each absorbed photon transfers momentum $\hbar k$ to the atom, so the average scattering force from one beam is

$$F_{\text{sc}} = \hbar k \, R_{\text{sc}}. \tag{23}$$

If two counter-propagating laser beams are used and the atom moves with velocity v, then the Doppler shift makes one beam closer to resonance and the other farther from resonance. For sufficiently small velocities, the net force becomes approximately linear:

$$F(v) \approx -\alpha v, \tag{24}$$

where $\alpha > 0$ is a damping coefficient. This is the basis of Doppler cooling.

4.2 Doppler Cooling Limit

Cooling by radiation pressure is accompanied by momentum diffusion from random spontaneous emission. Balancing damping and diffusion gives the Doppler temperature limit

$$T_D = \frac{\hbar \Gamma}{2 k_B}. \tag{25}$$

For alkali atoms this often lies in the range of a few hundred μK or below, depending on the transition linewidth.

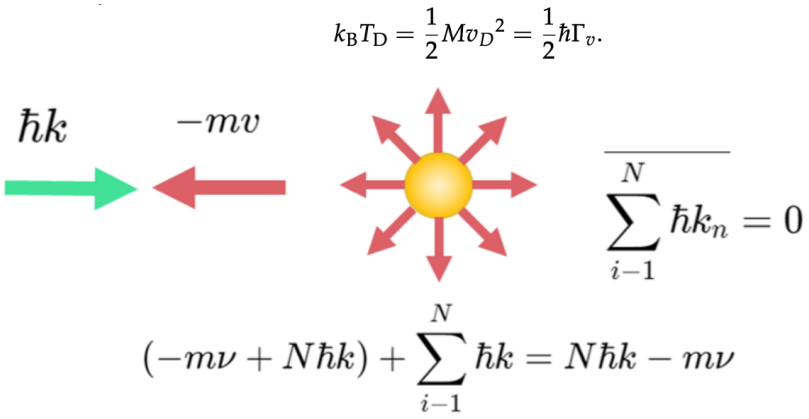

Figure 1. Physical diagram of Doppler cooling mechanism.

4.3 Magneto-Optical Trap (MOT)

A MOT combines Doppler cooling with a spatially restoring force. This is achieved using:

1. three orthogonal pairs of counter-propagating red-detuned laser beams,

2. a magnetic quadrupole field with a zero at the trap center.

Near the center of the trap, the magnetic field is approximately linear in position. For example, along one axis,

$$B(z) \approx b'z, \tag{26}$$

where b' is the magnetic-field gradient. Because of the Zeeman shift, the atomic resonance frequency depends on position. Together with the circular polarizations of the counter-propagating beams, this makes the atom preferentially absorb photons from the beam that pushes it back toward the center.

Thus the net force near the trap center can be written in the form

$$F(z, v) \approx -\kappa z - \alpha v, \tag{27}$$

where:

- $-\alpha v$ is the Doppler cooling term,
- $-\kappa z$ is the restoring force from the magnetic-field gradient and Zeeman shift.

This is formally similar to a damped harmonic oscillator, except that here the restoring and damping forces arise from light scattering.

Physical Insight

The MOT is the workhorse of neutral-atom experiments because it simultaneously cools and traps a large ensemble of atoms. It provides the cold atomic cloud from which single atoms are later loaded into microscopic tweezer traps.

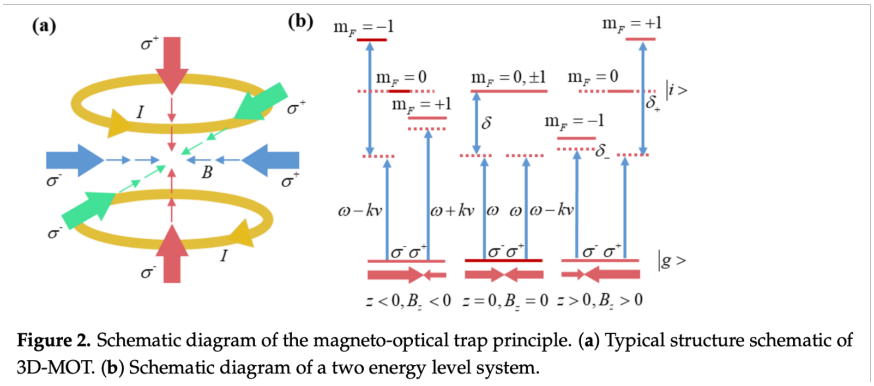

Figure 2. Schematic diagram of the magneto-optical trap principle. **(a)** Typical structure schematic of 3D-MOT. **(b)** Schematic diagram of a two energy level system.

4.4 Why the MOT Must Be Followed by Tweezers

Although the MOT provides cooling and localization, it is not suitable for precise single-site quantum control in large programmable arrays. The trapped cloud is too extended and too dissipative:

- the confinement volume is much larger than a single optical tweezer,
- the trapping relies on near-resonant scattering light, which causes continuous dissipation,
- individual atoms are not deterministically isolated at well-defined quantum-register sites.

Therefore, after MOT cooling, atoms are transferred into tightly focused far-off-resonant optical tweezers, where coherent control and single-site addressing become possible.

4.5 Loading from the MOT into Optical Tweezers

When a focused tweezer beam overlaps the cold MOT cloud, atoms can be captured if their kinetic energy is smaller than the tweezer depth. Loading is stochastic: each tweezer may contain zero, one, or more atoms initially. In many experiments, light-assisted collisions remove pairs of atoms, leaving predominantly single-atom occupancy.

This is the origin of *collisional blockade*, which helps prepare one atom per tweezer site with high probability.

Caution

A MOT is a dissipative, near-resonant cooling-and-capture stage for many atoms, whereas a tweezer is a conservative far-detuned microtrap used for single-atom confinement and coherent quantum control.

5. Optical Tweezers: Physical Basis

5.1 Dipole Interaction and AC Stark Shift

A neutral atom placed in an oscillating electric field develops an induced dipole moment. If the field is far detuned from resonance, the atom experiences an energy shift rather than strong absorption. This is the origin of the optical dipole trap.

Take a classical electric field

$$\mathbf{E}(t) = \mathbf{E}_0 \cos(\omega t). \tag{28}$$

The induced dipole is

$$\mathbf{p}(t) = \alpha(\omega)\mathbf{E}(t), \tag{29}$$

where $\alpha(\omega)$ is the dynamic polarizability. The instantaneous interaction energy is

$$U(t) = -\mathbf{p}(t) \cdot \mathbf{E}(t). \tag{30}$$

Time-averaging over an optical cycle gives

$$\langle U \rangle = -\frac{1}{2}\alpha(\omega)|E_0|^2. \tag{31}$$

Thus the optical dipole potential is

$$U(\mathbf{r}) = -\frac{1}{2}\alpha(\omega)|E(\mathbf{r})|^2. \tag{32}$$

5.2 Rewriting the Potential in Terms of Intensity

Using the intensity relation

$$I(\mathbf{r}) = \frac{1}{2}c\epsilon_0|E(\mathbf{r})|^2, \tag{33}$$

we obtain

$$|E(\mathbf{r})|^2 = \frac{2I(\mathbf{r})}{c\epsilon_0}. \tag{34}$$

Substituting into Eq. (32) yields

$$U(\mathbf{r}) = -\frac{1}{2}\alpha(\omega)\frac{2I(\mathbf{r})}{c\epsilon_0} \tag{35}$$

$$= -\frac{\alpha(\omega)}{c\epsilon_0}I(\mathbf{r}). \tag{36}$$

Depending on the convention used for complex amplitudes, one also often sees

$$U(\mathbf{r}) = -\frac{\alpha(\omega)}{2c\epsilon_0}I(\mathbf{r}), \tag{37}$$

with the factor of 2 absorbed into the field definition. The key physics is unchanged: the potential is proportional to intensity.

Remark

For red detuning, the polarizability leads to attraction toward large intensity, so atoms are trapped at the beam focus. For blue detuning, atoms are repelled from high intensity and can be trapped at intensity minima.

5.3 Far-Detuned Two-Level Approximation

For a two-level atom driven with detuning $\Delta = \omega - \omega_0$, the AC Stark shift in the far-detuned limit $|\Delta| \gg \Gamma, \Omega$ can be written as

$$U(\mathbf{r}) \approx \frac{3\pi c^2}{2\omega_0^3}\frac{\Gamma}{\Delta}I(\mathbf{r}). \tag{38}$$

The photon scattering rate is

$$\Gamma_{sc}(\mathbf{r}) \approx \frac{3\pi c^2}{2\omega_0^3}\frac{\Gamma^2}{\Delta^2}I(\mathbf{r}). \tag{39}$$

5.4 Derivation of the Useful Scaling

Comparing Eqs. (38) and (39), we see that

$$U \propto \frac{I}{\Delta}, \qquad \Gamma_{sc} \propto \frac{I}{\Delta^2}. \tag{40}$$

Therefore, increasing detuning while compensating with laser power allows one to maintain trap depth while reducing spontaneous scattering.

Physical Insight

This is a foundational design principle of optical tweezers: use a far-red-detuned, tightly focused beam so the atom experiences a deep trap but only weak photon-scattering-induced heating and decoherence.

6. Gaussian Beam Model of a Tweezer

6.1 Intensity Distribution

A diffraction-limited tweezer is well approximated by a focused Gaussian beam. Its intensity is

$$I(r,z) = \frac{2P}{\pi w(z)^2} \exp\left(-\frac{2r^2}{w(z)^2}\right), \tag{41}$$

where P is optical power and

$$w(z) = w_0\sqrt{1+\left(\frac{z}{z_R}\right)^2} \tag{42}$$

is the beam radius, with waist w_0 and Rayleigh range

$$z_R = \frac{\pi w_0^2}{\lambda}. \tag{43}$$

At the focus $z = 0$,

$$I(r,0) = \frac{2P}{\pi w_0^2} \exp\left(-\frac{2r^2}{w_0^2}\right). \tag{44}$$

Using $U \propto I$, the trapping potential is approximately

$$U(r,z) = U_0 \frac{w_0^2}{w(z)^2} \exp\left(-\frac{2r^2}{w(z)^2}\right), \tag{45}$$

where $U_0 < 0$ for a red-detuned trap. Often one quotes the trap depth as $|U_0|$.

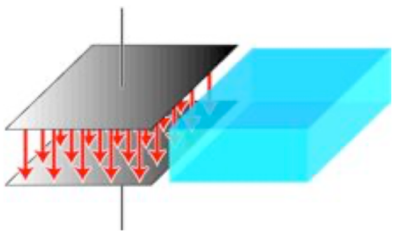

The charged capacitor
- "gradient force" acts on dielectric
- Draws dielectric into region of high field

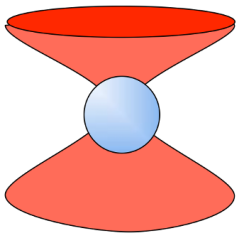

- The focused laser
  - "gradient force" acts on dielectric
  - Draws dielectric into region of high field
  - But need to immerse in fluid to damp motion

6.2 Harmonic Approximation Near the Trap Minimum

Near the trap center, the atom explores only a small region. Then the Gaussian potential can be expanded to quadratic order and approximated as a harmonic oscillator.

At $z = 0$,

$$U(r) = U_0 \exp\left(-\frac{2r^2}{w_0^2}\right). \tag{46}$$

For small r, use the Taylor series

$$e^{-x} \approx 1 - x + \frac{x^2}{2!} - \cdots . \tag{47}$$

With $x = 2r^2/w_0^2$,

$$U(r) \approx U_0 \left(1 - \frac{2r^2}{w_0^2}\right). \tag{48}$$

The harmonic oscillator potential is

$$U_{ho}(r) = U_0 + \frac{1}{2} m\omega_r^2 r^2. \tag{49}$$

Equating quadratic terms in magnitude gives

$$\frac{1}{2} m\omega_r^2 = \frac{2|U_0|}{w_0^2}, \tag{50}$$

so that

$$\omega_r = \sqrt{\frac{4|U_0|}{m w_0^2}}. \tag{51}$$

6.3 Axial Trap Frequency

Along the beam axis, set $r = 0$ and use

$$U(0, z) = U_0 \frac{1}{1 + (z/z_R)^2}. \tag{52}$$

For small z,

$$\frac{1}{1+x} \approx 1 - x, \qquad x = \left(\frac{z}{z_R}\right)^2, \tag{53}$$

thus

$$U(0, z) \approx U_0 \left(1 - \frac{z^2}{z_R^2}\right). \tag{54}$$

Compare with

$$U_{ho}(z) = U_0 + \frac{1}{2} m\omega_z^2 z^2. \tag{55}$$

Then

$$\frac{1}{2} m\omega_z^2 = \frac{|U_0|}{z_R^2}, \tag{56}$$

which gives

$$\omega_z = \sqrt{\frac{2|U_0|}{m z_R^2}}. \tag{57}$$

Caution

The radial confinement is much stronger than the axial confinement because typically $z_R \gg w_0$. Therefore a tweezer trap is anisotropic, with high transverse frequency and lower axial frequency.

7. Quantum Motion in the Tweezer

Once the trap is approximated as harmonic, the motional Hamiltonian is

$$H_{mot} = \hbar\omega \left(a^\dagger a + \frac{1}{2} \right), \tag{58}$$

with eigenenergies

$$E_n = \hbar\omega \left(n + \frac{1}{2} \right), \qquad n = 0, 1, 2, \ldots \tag{59}$$

The spatial extent of the ground state is

$$x_0 = \sqrt{\frac{\hbar}{2m\omega}}. \tag{60}$$

7.1 Lamb-Dicke Regime

Define the Lamb-Dicke parameter

$$\eta = k x_0, \tag{61}$$

where $k = 2\pi/\lambda$ is the optical wave number of the addressing beam. The Lamb-Dicke regime is

$$\eta \ll 1. \tag{62}$$

In this regime, recoil during photon absorption/emission does not strongly change the motional state. This is important for sideband cooling and high-fidelity coherent control.

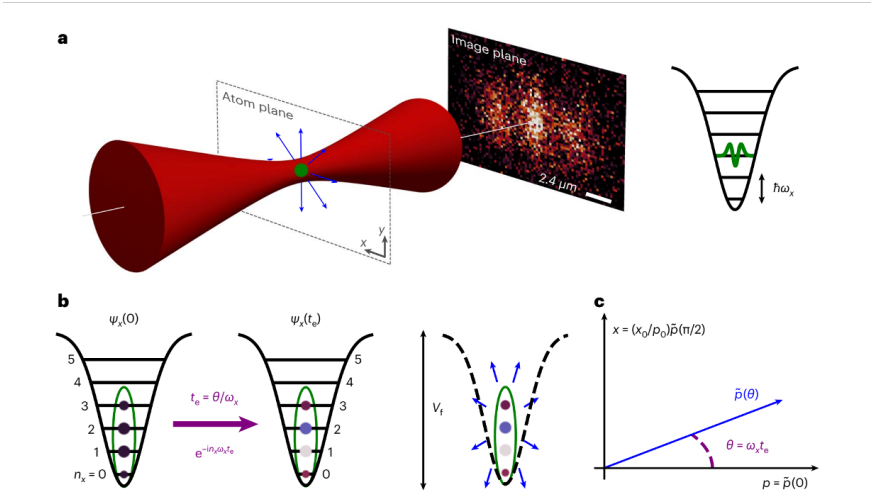

8. Heating, Scattering, and Technical Noise

The ideal trap should be deep, quiet, and weakly scattering. In practice, motional excitation arises from several sources:

1. photon recoil from off-resonant scattering,
2. laser intensity noise,
3. beam pointing noise,

4. phase or frequency noise of addressing beams,
5. background gas collisions.

A common qualitative statement is that parametric heating is sensitive to trap-frequency-band noise. If the fractional intensity noise has spectral density $S_I(2\omega)$ near twice the trap frequency, the heating rate scales like

$$\dot{n} \propto S_I(2\omega). \tag{63}$$

This is why quiet laser power stabilization matters.

Remark

In lecture, it is useful to separate two very different limitations:

- **fundamental:** photon scattering from the finite detuning of the trap light,
- **technical:** classical noise in the trapping optics.

Students often mix these together, but they scale differently and are mitigated differently.

9. Tweezer Arrays: From One Trap to Many

A single tweezer already demonstrates single-atom trapping physics, but scalable quantum science requires many tweezers. Two common beam-shaping routes are:

1. **Spatial light modulators (SLM):** create static or programmable multi-site intensity patterns.
2. **Acousto-optic deflectors (AOD):** rapidly steer beams to form static or time-averaged arrays and enable dynamical rearrangement.

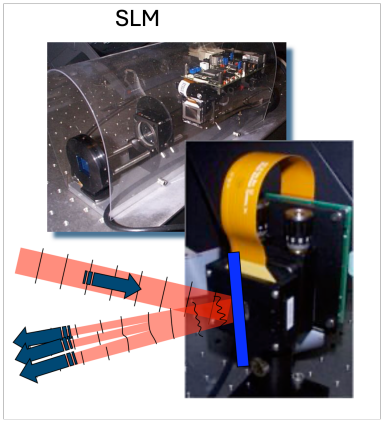

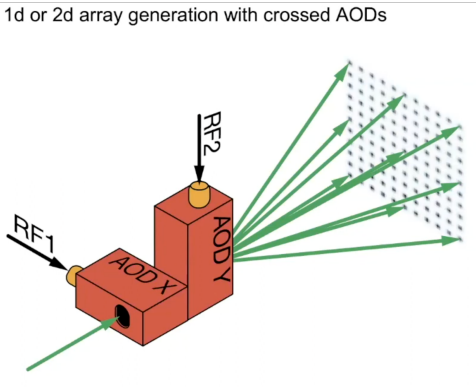

9.1 Defect-Free Rearrangement

Stochastic loading typically leaves vacancies. A major breakthrough in neutral-atom arrays is measurement-based rearrangement: image which sites are occupied, then move occupied tweezers to desired target positions. This converts probabilistic loading into a nearly defect-free register.

10. Single-Qubit and Rydberg-Coupled Dynamics

10.1 Two-Level Driven Atom

For one atom with qubit states or ground–Rydberg states coupled by a resonant laser, the rotating-frame Hamiltonian is

$$H = \frac{\hbar\Omega}{2}\sigma_x - \frac{\hbar\Delta}{2}\sigma_z. \tag{64}$$

On resonance ($\Delta = 0$), the time evolution produces Rabi oscillations:

$$P_e(t) = \sin^2\left(\frac{\Omega t}{2}\right). \tag{65}$$

10.2 Controlled Phase from Blockade

The interaction-shifted state $|rr\rangle$ allows conditional dynamics. In the strong blockade regime, the two-atom system avoids double excitation and acquires state-dependent phases. This is the basis of controlled-phase and CNOT-like gate constructions.

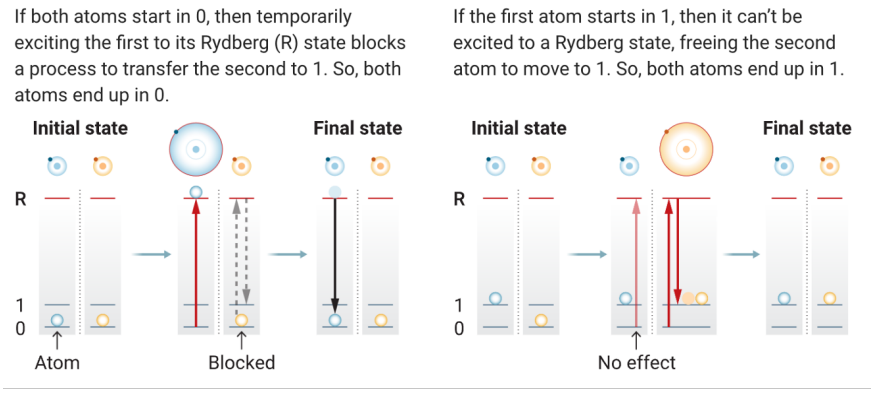

11. Quantum Computing with Rydberg Atoms

Rydberg-atom platforms are one of the leading approaches to quantum computing because they combine:

1. long-lived ground-state qubits,
2. strong and switchable two-qubit interactions,
3. natural scalability in two-dimensional tweezer arrays,
4. optical initialization, manipulation, and readout.

The basic idea is simple: atoms are stored in weakly interacting ground states most of the time, and strong interactions are turned on only temporarily by exciting one or both atoms to a Rydberg level. This allows one to implement both single-qubit gates and entangling two-qubit gates in a programmable architecture.

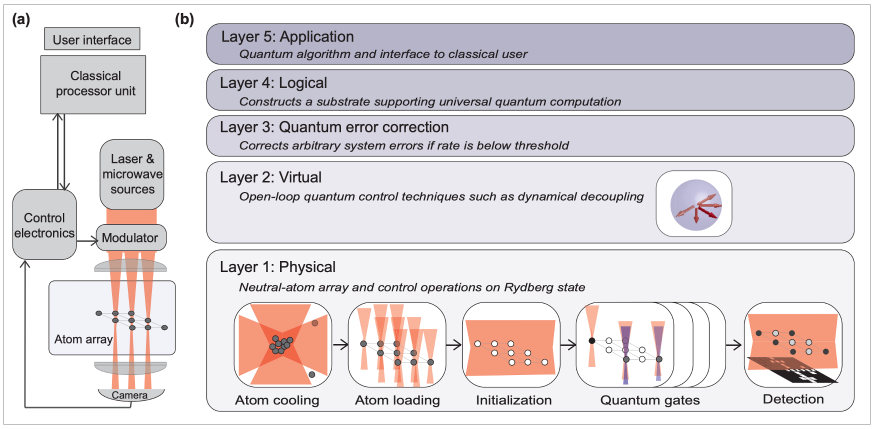

11.1 Qubit Encoding

A neutral-atom qubit is usually encoded in two long-lived internal states, often hyperfine ground states:

$$|0\rangle \equiv |g_0\rangle\,, \qquad |1\rangle \equiv |g_1\rangle\,. \tag{66}$$

Because both states are low-lying atomic states, they can have long coherence times and relatively weak sensitivity to unwanted interactions.

Single-qubit control is achieved by resonant microwave, Raman, or optical coupling between these two states. In the rotating frame, the driven single-qubit Hamiltonian can be written as

$$H_{1q} = \frac{\hbar\Omega}{2}\sigma_x - \frac{\hbar\Delta}{2}\sigma_z, \tag{67}$$

where Ω is the Rabi frequency and Δ is the detuning.

On resonance, $\Delta = 0$, the atom undergoes coherent Rabi oscillations:

$$P_1(t) = \sin^2\left(\frac{\Omega t}{2}\right). \tag{68}$$

Remark

The ground-state qubit provides storage, while the Rydberg state provides interaction. This separation of roles is one of the most attractive features of the platform.

11.2 Why Rydberg Excitation Enables Two-Qubit Gates

Two atoms in their qubit ground states interact only weakly. However, if one attempts to excite them to a Rydberg state, the interaction energy of the doubly excited state can become very large:

$$V(R) = \frac{C_6}{R^6} \quad \text{or} \quad V(R) = \frac{C_3}{R^3}, \tag{69}$$

depending on the regime.

When the interaction shift satisfies

$$V(R) \gg \hbar\Omega, \tag{70}$$

the state $|rr\rangle$ is shifted out of resonance. As a result, the excitation of one atom can block the excitation of a nearby second atom. This is the Rydberg blockade mechanism, and it produces the conditional dynamics needed for entangling quantum gates.

11.3 Controlled-Phase Gate Idea

A standard two-qubit gate based on blockade is the controlled-phase (CZ) gate. The logic is that one atom acts as a control and the second as a target. If the control atom is transferred to a Rydberg state, it shifts the target atom out of resonance and changes the target's dynamical phase evolution.

Schematically, the ideal CZ gate acts as

$$|00\rangle \to |00\rangle\,, \tag{71}$$
$$|01\rangle \to |01\rangle\,, \tag{72}$$
$$|10\rangle \to |10\rangle\,, \tag{73}$$
$$|11\rangle \to -|11\rangle\,. \tag{74}$$

This phase flip is sufficient, together with single-qubit rotations, to form a universal gate set.

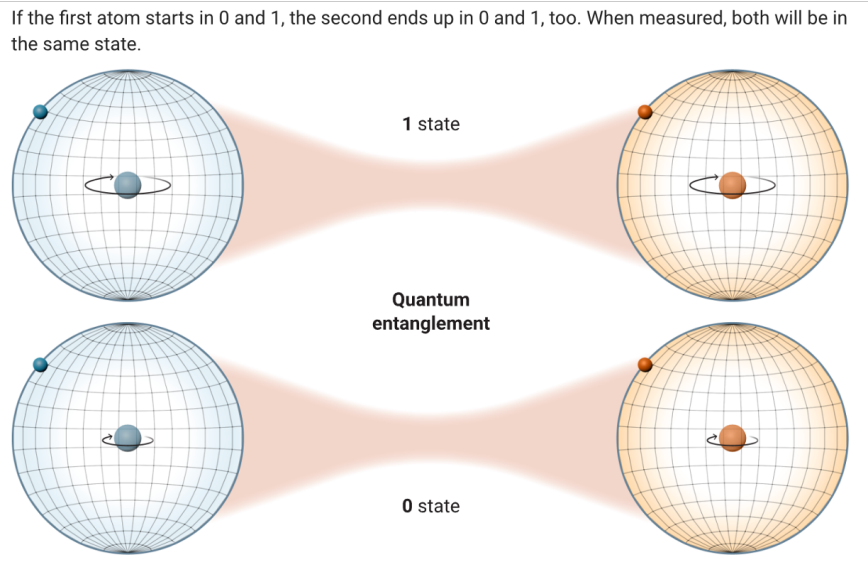

11.4 Minimal Physical Picture of a Blockade Gate

A simplified gate sequence can be understood in three steps:

1. Apply a π pulse to transfer the control qubit state $|1\rangle$ to a Rydberg state $|r\rangle$.
2. Apply a 2π pulse on the target atom.
3. De-excite the control atom back to the qubit manifold.

If the control atom is not in the state that gets excited, the target undergoes its intended cyclic evolution and acquires a phase. If the control atom *is* in the Rydberg state, blockade prevents the target excitation, so the phase evolution is different. The final result is a state-dependent phase, i.e. an entangling gate.

Physical Insight

The key principle is conditional resonance: the target atom behaves differently depending on whether the control atom has already been promoted to a Rydberg state.

11.5 Why the Platform Scales Well

Optical tweezer arrays are naturally suited to large quantum registers:

1. atoms can be trapped in one- or two-dimensional geometries,
2. empty sites can be corrected by rearrangement,
3. local optical addressing can be combined with global illumination,
4. the geometry itself can be programmable.

This makes the platform useful not only for digital gate-based quantum computing, but also for analog quantum simulation. In analog mode, one engineers a many-body Hamiltonian directly. In digital mode, one composes a sequence of quantum gates.

11.6 Analog and Digital Operation

In analog quantum simulation, one exploits the natural interacting Hamiltonian of a Rydberg array. A common effective model is

$$H = \sum_i \frac{\hbar\Omega_i}{2}\sigma_i^x - \sum_i \frac{\hbar\Delta_i}{2}\sigma_i^z + \sum_{i<j} V_{ij} n_i n_j, \tag{75}$$

where

$$n_i = \frac{1+\sigma_i^z}{2} \tag{76}$$

represents the Rydberg occupation on site i.

Here we use the convention that $\sigma_i^z |r\rangle_i = +|r\rangle_i$ and $\sigma_i^z |g\rangle_i = -|g\rangle_i$, so that $n_i = (1+\sigma_i^z)/2$ projects onto the Rydberg state.

This Hamiltonian describes coherent driving, detuning, and interaction-induced energy shifts. It is central both to many-body physics experiments and to programmable neutral-atom processors.

In digital gate-based computing, the goal is instead to implement a universal gate set, such as:

1. arbitrary single-qubit rotations,
2. one entangling two-qubit gate, such as CZ or CNOT.

Once these are available with sufficiently low error, arbitrary quantum circuits can in principle be compiled.

11.7 Strengths and Challenges

The main strengths of Rydberg-atom quantum computing are:

1. strong and controllable entangling interactions,
2. high connectivity within the blockade range,
3. reconfigurable geometry,
4. direct compatibility with large atom arrays.

At the same time, several challenges remain:

1. finite Rydberg-state lifetime,
2. laser phase noise and intensity noise,
3. motional dephasing,
4. imperfect state preparation and detection,
5. gate errors from incomplete blockade or off-resonant excitation.

Caution

A large interaction strength alone does not guarantee a high-fidelity quantum computer. One must also control technical noise, spontaneous decay, addressing errors, and atom loss across the full experimental sequence.

11.8 Conceptual Summary

Rydberg-atom quantum computing rests on a clear division of tasks:

- the ground-state manifold stores quantum information,
- optical tweezers provide trapping and register geometry,
- laser pulses provide coherent control,
- Rydberg excitation provides tunable interactions,
- blockade converts interaction into entangling logic.

This combination of long-lived qubits, programmable geometry, and strong conditional interactions is what makes the platform so powerful.

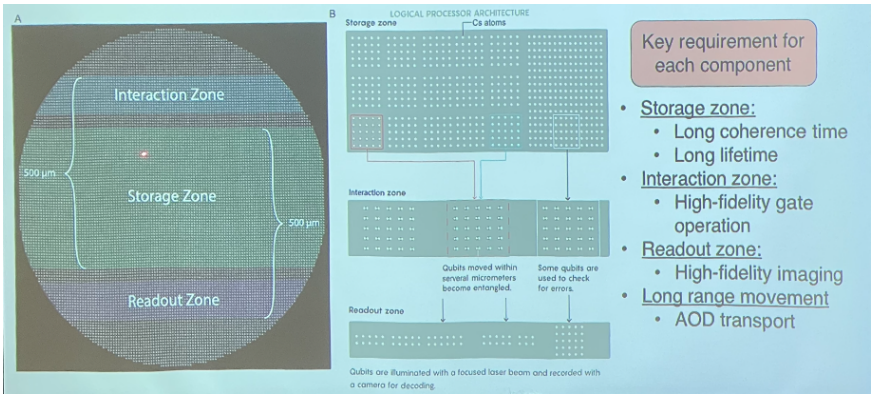

12. References

[1] M. Endres, *Quantum Science with Tweezer Arrays*, lecture, March 11, 2021. `https://www.youtube.com/watch?v=l40-BmccemQ`

[2] T. F. Gallagher, *Rydberg Atoms*, Rev. Mod. Phys. **70**, 721 (1998).

[3] S. Bao *et al.*, *Rydberg-Atom-Based Quantum Technologies*, Photonics **12**, 98 (2025). https://doi.org/10.3390/photonics12020098

[4] M. O. Brown *et al.*, *Quantum simulation of spin models with Rydberg atoms*, Nat. Phys. **19**, 569–573 (2023). https://doi.org/10.1038/s41567-022-01890-8

[5] X. Wu *et al.*, *A concise review of Rydberg atom based quantum computation and quantum simulation*, arXiv:2012.10614 (2021).

[6] H. J. Manetsch *et al.*, *Programmable quantum simulation with Rydberg atom arrays*, Nature **647**, 60–67 (2025). https://doi.org/10.1038/s41586-025-09641-4

[7] O. Ezratty, *Understanding Quantum Technologies*, 2025 edition. https://www.oezratty.net/wordpress/quantum/understanding-quantum-technologies/